Antibacterial Effectiveness of Zinc Oxide and Magnesium Oxide Nanoparticles Against *Enterococcus faecalis*: An *In Vitro* Study

Srilekha Jayakumar[1], Ramaprabha Balasubramanian[2], Nandhini Ambalavanan[2], Anbarasu Subramanian[3], H. Shalini[4], Raja Chandrasekaran[5]

[1]Department of Conservative Dentistry and Endodontics, Chettinad Dental College and Research Institute, Kelambakkam, Chengalpettu, [2]Tamil Nadu Government Dental College and Hospital, The Tamil Nadu Dr. MGR Medical University, Chennai, [3]Department of Dentistry, Government Mohan Kumaramangalam Medical College, The Tamilnadu Dr. MGR Medical University, Salem, [4]Department of Conservative Dentistry and Endodontics, Sree Balaji Dental College and Hospital, Bharath Institute of Higher Education and Research, Chennai, Tamil Nadu, [5]Department of Dentistry, Military Dental Center, Meerut, Uttar Pradesh, India

Abstract

Background: Persistent endodontic infections, often attributed to *Enterococcus faecalis*, pose a significant challenge to successful root canal treatment. Conventional disinfection methods have limitations in eradicating bacteria within complex root canal anatomy. Nanoparticles (NPs) have evolved as favorable antibacterial agents due to their distinctive properties. **Aim:** To compare the antimicrobial activity of ZnO and MgO NPs (nanorods and nanospheres) with 3% sodium hypochlorite (NaOCl) against *E. faecalis* (American-type culture collection [ATCC] 29212 and a clinical oral isolate) using agar well diffusion, minimum inhibitory concentration (MIC), and time-kill assays. **Methods:** ZnO and MgO NPs (nanorods and nanospheres) were synthesized and characterized using ultraviolet-visible (UV-visible) spectrophotometry to determine the optical properties of materials and transmission electron microscopy for measuring nanoparticle size, distribution, morphology, and grain size. Agar well diffusion was used to measure antimicrobial activity at various volumes (50–150 µL). MIC was calculated using the broth microdilution method. Time-kill assays were performed by quantifying colony-forming units at 15 min intervals for 90 min. One-way analysis of variance with Tukey's *post hoc* test ($P < 0.05$) was used for statistical analysis. **Results:** The peak acquired for ZnO nanorods was 360 nm, ZnO nanosphere was 350 nm, MgO nanorods were 250 nm, and MgO nanosphere was 270 nm in UV-visible spectrophotometry. The transmission electron microscope confirmed an average NP size of 20 nm for all morphologies. In the agar well diffusion assay, ZnO nanorods exhibited better activity than other NPs except for 3% NaOCl against both *E. faecalis* strains at all volumes (75–150 µL) ($P = 0.001$). MgO nanorods also demonstrated significant activity, although generally at higher volumes (150 µL) than ZnO ($P = 0.001$) and MgO ($P = 0.002$) nanospheres. The MIC values (mg/mL) against the ATCC strain were as follows: MgO-S (1.17), MgO-R (18.75), ZnO-R (18.75), and ZnO-S (37.5). Against the clinical isolate, the MIC values were as follows: MgO-R (18.5), MgO-S (18.5), ZnO-R (37.5), and ZnO-S (75). In the time-kill assay, all NPs, except MgO nanorods against the ATCC strain (effective at 30 min), achieved rapid bactericidal activity within 15 min, comparable to 3% NaOCl. **Conclusion:** Both ZnO and MgO NPs, particularly ZnO nanorods, demonstrated promising antimicrobial activity against *E. faecalis in vitro*, comparable to 3% NaOCl in certain assays. ZnO NPs of various shapes have distinct active facets that increase their antimicrobial action such as rods and wires that have more facets than spherical NPs. ZnO nanorods penetrate easily into the cell walls of bacteria than nanosphere. Additionally, ZnO nanorod and sphere release more reactive oxygen species (ROS) that interacts with proteins, resulting in bacterial cell lysis. The main mechanism of action of MgO NPs (nanorod and nanosphere) is the formation of ROS that interacts with the proteins peptide linkages in microorganisms, ultimately resulting in cell death. These results highlight the potential of these NPs in endodontic disinfection, such as incorporation into sealers or gutta-percha coatings. Future research should focus on evaluating their biocompatibility and long-term efficacy in biofilm models.

Address for correspondence: Dr. Srilekha Jayakumar, Department of Conservative Dentistry and Endodontics, Chettinad Dental College and Research Institute, Kelambakkam, Chengalpettu 603103, Tamil Nadu, India.
E-mail: srilekhajayakumar@gmail.com

How to cite this article: Jayakumar S, Balasubramanian R, Ambalavanan N, Subramanian A, Shalini H, Chandrasekaran R. Antibacterial effectiveness of zinc oxide and magnesium oxide nanoparticles against *Enterococcus faecalis*: An *in vitro* study. J Int Oral Health 2025;17:96-105.

Access this article online

Quick Response Code:

Website: www.jioh.org

DOI: 10.4103/jioh.jioh_164_24

Keywords: Alkaline Effect, *Enterococcus faecalis*, Nanorods, Nanosphere, Reactive Oxygen Species, Zinc Oxide Nanoparticles

Received: 20-Jul-2024, **Revised:** 12-Jan-2025, **Accepted:** 20-Jan-2025, **Published:** 30-Apr-2025.

Introduction

Eliminating bacteria from the root canal system and preventing re-infection are the two key factors that determine the success of endodontic treatment.[1] The complexity of root canal morphology, the presence of organic debris, and microbes, that is, located deep inside the dentinal tubules render it challenging to maintain a root canal free of microbes.[2,3] In the root canal system, bacteria may exist as single, free-floating planktonic cells or in the form of a biofilm.[4,5]

Enterococcus faecalis is the predominant microbe in post-treatment apical periodontitis, which has frequently been identified in pure culture from the root canal system. It has been shown that *E. faecalis* demonstrates extensive genetic polymorphisms and overcomes survival constraints in different ways.[6] It owns various virulence factors such as aggregation substance, cytolysin, polyamines, serine protease, gelatinase, and collagen-binding protein.[7] It can endure prolonged periods of starvation by existing in a viable but not cultivable state until a sufficient quantity of nutrients is available. A proton pump found in *E. faecalis* offers a way to preserve pH homeostasis within the cell when exposed to an alkaline environment.[8,9]

Currently, mechanical debridement and chemical disinfection are employed to treat endodontic infections. Clinical research, however, has demonstrated that bacteria continue to exist in the uninstrumented portions and intricate regions of the root canals even after thorough chemo-mechanical debridement and obturation.[10,11] Studies have reported a reduction in the microhardness of dentin when sodium hypochlorite (NaOCl) is used in various concentrations.[12] In addition, NaOCl lacks substantivity and is unable to remove the smear layer.[13,14] Other root canal irrigants, like chlorhexidine gluconate (CHX), are unable to dissolve pulp tissues. Furthermore, both NaOCl and CHX have limited ability to penetrate dentinal tubules, respectively.[15] The use of nanoparticles (NPs) in endodontic disinfection is a novel approach to enhance disinfection strategies, that is, being researched and investigated due to the aforementioned drawbacks of current anti-biofilm approaches in root canal treatment.[16,17]

NPs are tiny particles that range in size from 1 to 100 nm. They are known to possess characteristics that set them apart from their bulk or powdered counterparts. It has been discovered that antibacterial NPs exhibit a wide range of antimicrobial action and have a lower incidence of developing microbial resistance.[18] In addition, NPs are considered a potential game-changer in the field of endodontics via their wide applications. However, in both microscale and nanoscale formulations, zinc oxide and magnesium oxide NPs are now being explored as antibacterial agents.[19-23] This study aimed to investigate the antibacterial efficacy of zinc oxide and magnesium oxide NPs with two distinct shapes such as nanorod and nanosphere against *E. faecalis*.

Materials and Methods

Synthesis of nanoparticles

All the materials required for the synthesis of NPs were obtained from Sigma-Aldrich, Germany.

Preparation

Zinc oxide nanorods (ZnO-R) were prepared by using zinc hydroxide as a precursor in an alcohol solution through a hydrothermal technique.[24] Zinc oxide nanospheres (ZnO-S) were synthesized using a simple sol-gel technique with zinc chloride, zinc nitrate, and sodium hydroxide as starting materials at room temperature.[25] Magnesium oxide nanorods (MgO-R), on the other hand, were synthesized using polyethylene glycol 600 (PEG 600) as a template in the co-precipitation method.[26] Magnesium oxide (MgO-S) NPs were synthesized using a sol-gel process utilizing magnesium nitrate and sodium hydroxide.[27]

Characterization of nanoparticles

An ultraviolet-visible spectrophotometer was used to assess the distinctive absorbance peak of the prepared NPs to determine the optical properties of materials, in terms of specific wavelengths they absorb, scatter, and reflect, and analyze its stability. The peak obtained for ZnO-Rs was 360 nm, ZnO-S was 350 nm, MgO-Rs was 250 nm, and magnesium oxide nanosphere was 270 nm. The NPs were further evaluated using a transmission electron microscope (TEM) (Tecnai) for measuring nanoparticle size, distribution, morphology, and grain size. NPs were 20 nm in size on average, and their morphology, nanorod and nanosphere, was evaluated using TEM [Figure 1].

Microbiological analysis

Bacterial strains evaluated in the study

Standard strain: The *E. faecalis* American-type culture collection (ATCC) 29212 freeze-dried ampoule was purchased from HiMedia Laboratories Pvt. Ltd. in India.

Oral isolate: A stock culture of an oral isolate strain of *E. faecalis* was identified and preserved from the root canal of a patient who had failed root canal therapy.

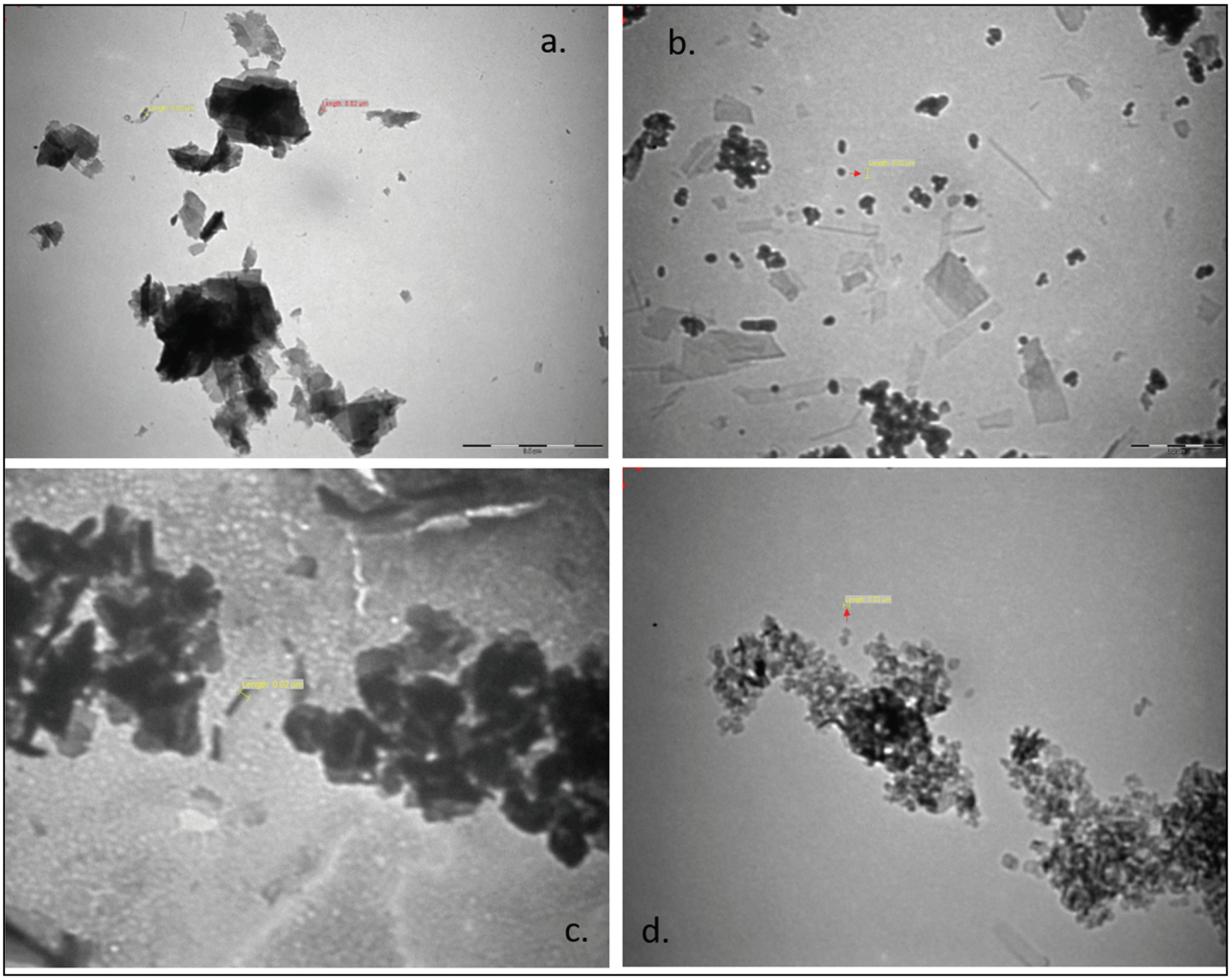

Figure 1: Characterized nanoparticles of (a.) zinc oxide nanorods, (b.) zinc oxide nanospheres, (c.) magnesium oxide nanorods, and (d.) magnesium oxide nanospheres

Revival of E. faecalis

A total of 500 µL of sterile saline was used to reconstitute the freeze-dried culture of *E. faecalis* ATCC 29212 strain. Using a sterile micropipette, 10 µL of the reconstituted bacterial culture was pipetted out and seeded onto sterile MacConkey agar plates. A total of 10 µL of sterile Mueller–Hinton broth was used to resuscitate the *E. faecalis* oral isolate stock culture, which was then subcultured on sterile MacConkey agar plates. Following a 24 h incubation period at 37°C, colony morphology was evaluated on the plates.

Inoculum preparation – ATCC 29212 strain and clinical isolate strain:

The cell densities of the isolated colonies of both strains were adjusted to 1.5 × 108 cfu/mL, that is, 0.5 Mcfarland standard or scale and suspended in sterile Mueller–Hinton broth in separate test tubes.

Preparation of the test solutions

NP stock solutions were made at a concentration of 100 mg/mL in 10% dimethyl sulfoxide (DMSO). The concentration of NPs was optimized using the methods described by Nkemzi *et al*.[28] A vortex mixer was used to evenly suspend the NPs. A total of 10% DMSO served as the negative control, and 3% sodium hypochlorite served as the positive control. The volumes assessed are 50, 75, 100, 125, and 150 µL, and the groups are as follows:

Group 1: 10% DMSO, Group 2: ZnO-R, Group 3: ZnO-S, Group 4: MgO-R, Group 5: MgO-S, and Group 6: 3% NaOCl.

Antibacterial activity of the test solutions (agar well diffusion method)

Separate Mueller–Hinton agar (MHA) plates were used to cultivate the lawn culture of the clinical isolate strain and ATCC 29212 strain of *E. faecalis*. With a sterile cork bore, wells with a diameter of 8 mm were punched. After adding 25, 50, 100, 125, and 150 µL of the test solutions (Group 1 to Group 6) to the correspondingly labeled wells, the plates were incubated for 24 h at 37°C. Following incubation, the diameter of the zone of inhibition surrounding the wells was measured in millimeters using the Hi antibiotic zone

scale-C (Hi Media Laboratories Pvt. Ltd., India). The test was performed in triplicates.[29]

Evaluation of minimum inhibitory concentration of the nano-suspensions

In accordance with the 2017 criteria of the Clinical Laboratory Standards Institute, the minimum inhibitory concentration (MIC) of the test solutions was ascertained using the broth microdilution method in sterile disposable 96-well microtiter plates (Zellkulter, Germany). The test solutions were serially diluted twice to determine the MIC for each group. The plates were incubated at 37°C for 18 h. The lowest concentration of the test solution that inhibits bacterial growth was noted as the MIC (no visible turbidity).

Time-kill assay

The time-kill assay is based on the rate at which a bacterial isolate is killed over a predetermined amount of time by being exposed to a specific concentration of the antimicrobial agent in a broth medium. The amount of exposure time needed to destroy a standardized microbial inoculum was calculated as the killing time. Cell densities were set to 1.5 × 108 cfu/mL after overnight cultures of *E. faecalis* ATCC 29212 and *E. faecalis* clinical isolate in MacConkey agar plate cultures were suspended in 1 mL of the test solutions (Groups 1 through 6) in different Eppendorf tubes. A total of 10 µL of the culture from each tube was pipetted out at 15 min intervals after the tubes were incubated at 37°C for 15, 30, 45, 60, 75, and 90 min. The spread plate method was used to seed the inoculum onto MHA plates. A digital colony counter was used to count the colony-forming unit following incubation. To determine the rate of killing, the number of viable bacteria was plotted over time. The acquired data were tabulated and statistically analyzed using SPSS for Windows (SPSS ver 22.0, IBM Corp., Armonk). Comparison of data between groups was evaluated using one-way analysis of variance with Tukey's *post hoc* test.

Results

American-type culture collection strain

Among NPs, the antibacterial activity of ZnO nanorods was significantly better than the negative control, ZnO-S, MgO-R, and MgO-S ($P = 0.001$) at all volumes (75–150 µL). However, 3% NaOCl had the highest antibacterial activity compared to all NPs at all volumes. At higher volumes (125 and 150 µL), MgO nanorods had significantly better antibacterial activity compared to ZnO nanospheres than MgO nanospheres ($P = 0.001$), respectively. The mean value of DMSO was significantly lower at all volumes. At 150 µL, the mean values of ZnO-S and MgO-S were comparable [Graph 1, Table 1].

For oral isolate

Among all NPs, ZnO nanorods had the highest antibacterial activity than ZnO nanospheres, MgO nanospheres, and nanorods that was statistically significant ($P = 0.001$) at all volumes (75–150 µL). However, 6.3% NaOCl had the highest antibacterial activity compared to all NPs at all volumes. At higher volumes (125 and 150 µL), MgO nanorods had significantly better antibacterial activity compared to ZnO nanospheres than MgO nanospheres ($P = 0.001$), respectively. The mean value of DMSO was significantly lower at all volumes. At 150 µL, the mean values of ZnO-S and MgO-S were comparable [Graph 2, Table 2].

Minimum inhibitory concentration

American-type culture collection strain

It was found that MgO-S was efficient at a lesser concentration of 1.17 mg/mL, followed by MgO-R and ZnO-R, which were effective at 18.75 mg/mL, while ZnO-S was effective at a concentration of 37.5 mg/mL against ATCC 29212 strain [Graph 3].

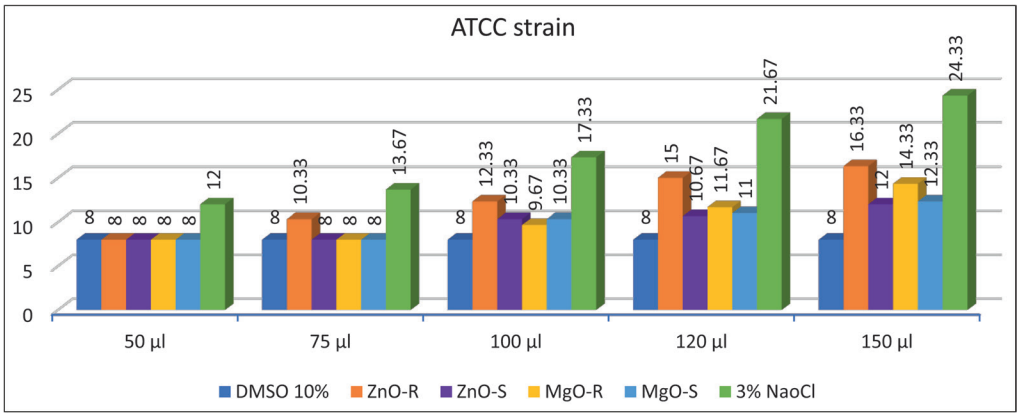

Graph 1: Mean zone of inhibition of all groups against American-type culture collection strain at different volumes

Table 1: Comparison of American-type culture collection strain between groups at different volumes using one-way analysis of variance

Concentration	Groups	Mean	SD	*F*	*P* value
50 µL	Dimethyl sulfoxide (DMSO) 10%	8.0	0.0	–	–
	Zinc oxide nanorods	8.0	0.0		
	Zinc oxide nanospheres	8.0	0.0		
	Magnesium oxide nanorods	8.0	0.0		
	Magnesium nanospheres	8.0	0.0		
	3% sodium hypochlorite	12.0	0.0		
75 µL	DMSO 10%	8.00^{abc}	0.0	145.2	<0.001*
	Zinc oxide nanorods	10.33	0.58		
	Zinc oxide nanospheres	8.0^{ade}	0.0		
	Magnesium oxide nanorods	8.0^{bdf}	0.0		
	Magnesium nanospheres	8.0^{cef}	0.0		
	3% sodium hypochlorite	13.67	0.58		
100 µL	DMSO 10%	8.0^{a}	0.0	71.4	<0.001*
	Zinc oxide nanorods	12.33	0.58		
	Zinc oxide nanospheres	10.33^{b}	0.58		
	Magnesium oxide nanorods	9.67^{abc}	0.58		
	Magnesium nanospheres	10.33^{bc}	0.58		
	3% sodium hypochlorite	17.33	1.15		
125 µL	DMSO 10%	8.00	0.00	415.2	<0.001*
	Zinc oxide nanorods	15.00	0.00		
	Zinc oxide nanospheres	10.67^{ab}	0.58		
	Magnesium oxide nanorods	11.67^{ac}	0.58		
	Magnesium nanospheres	11.00^{bc}	0.00		
	3% sodium hypochlorite	21.67	0.58		
150 µL	DMSO 10%	8.00	0.0	413.8	<0.001*
	Zinc oxide nanorods	16.33	0.58		
	Zinc oxide nanospheres	12.0^{a}	0.0		
	Magnesium oxide nanorods	14.33	0.58		
	Magnesium nanospheres	12.33^{a}	0.58		
	3% sodium hypochlorite	24.33	0.58		

^{a,b,c}are used to show which "Means" are significantly different from each other based on post-hoc tests. These annotations help in understanding which groups have statistically significant differences in a study.
*denotes statistically significant.

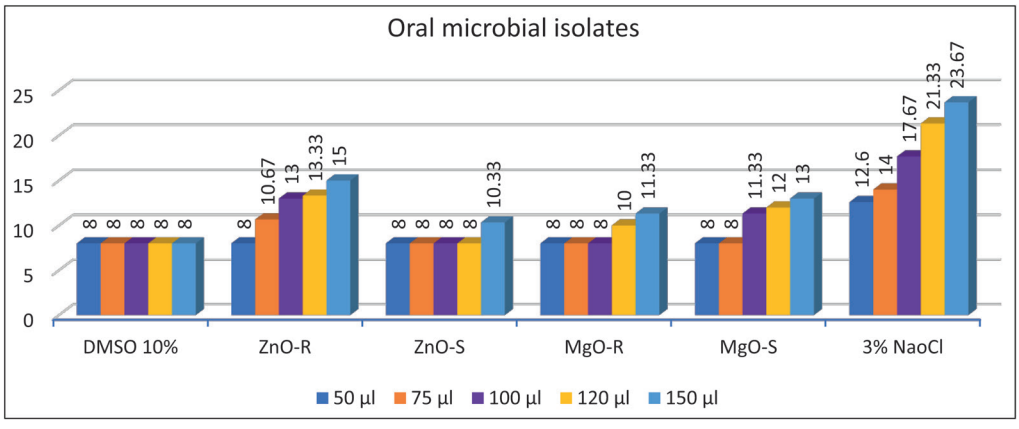

Graph 2: Mean zone of inhibition of all groups against oral isolate strain at different volumes

Table 2: Comparison of clinical oral isolate between groups at different volumes using one-way analysis of variance

Concentration	Groups	Mean	SD	*F*	*P* value
50 µL	Dimethyl sulfoxide (DMSO) 10%	8.0[abcd]	0.00	196.0	<0.001*
	Zinc oxide nanorods	8.0[aefg]	0.00		
	Zinc oxide nanospheres	8.0[behi]	0.00		
	Magnesium oxide nanorods	8.0[cfhj]	0.00		
	Magnesium nanospheres	8.0[dgij]	0.00		
	3% sodium hypochlorite	12.67	0.58		
75 µL	DMSO 10%	8.0[abc]	0.00	330.0	<0.001*
	Zinc oxide nanorods	10.67	0.58		
	Zinc oxide nanospheres	8.0[ade]	0.00		
	Magnesium oxide nanorods	8.0[bdf]	0.00		
	Magnesium nanospheres	8.0[cef]	0.00		
	3% sodium hypochlorite	14.0	0.00		
100 µL	DMSO 10%	8.0[ab]	0.00	408.0	<0.001*
	Zinc oxide nanorods	13.0	0.00		
	Zinc oxide nanospheres	8.0[ac]	0.00		
	Magnesium oxide nanorods	8.0[bc]	0.00		
	Magnesium nanospheres	11.33	0.58		
	3% sodium hypochlorite	17.67	0.58		
125 µL	DMSO 10%	8.0[a]	0.00	674.0	<0.001*
	Zinc oxide nanorods	13.33	0.58		
	Zinc oxide nanospheres	8.0[a]	0.00		
	Magnesium oxide nanorods	10.0	0.00		
	Magnesium nanospheres	12.0	0.00		
	3% sodium hypochlorite	21.33	0.58		
150 µL	DMSO 10%	8.00	0.00	542.2	<0.001*
	Zinc oxide nanorods	15.00	0.00		
	Zinc oxide nanospheres	10.33[a]	0.58		
	Magnesium oxide nanorods	11.33[a]	0.58		
	Magnesium nanospheres	13.00	0.00		
	3% sodium hypochlorite	23.67	0.58		

[a,b,c]are used to show which "Means" are significantly different from each other based on post-hoc tests. These annotations help in understanding which groups have statistically significant differences in a study.
*denotes statistically significant.

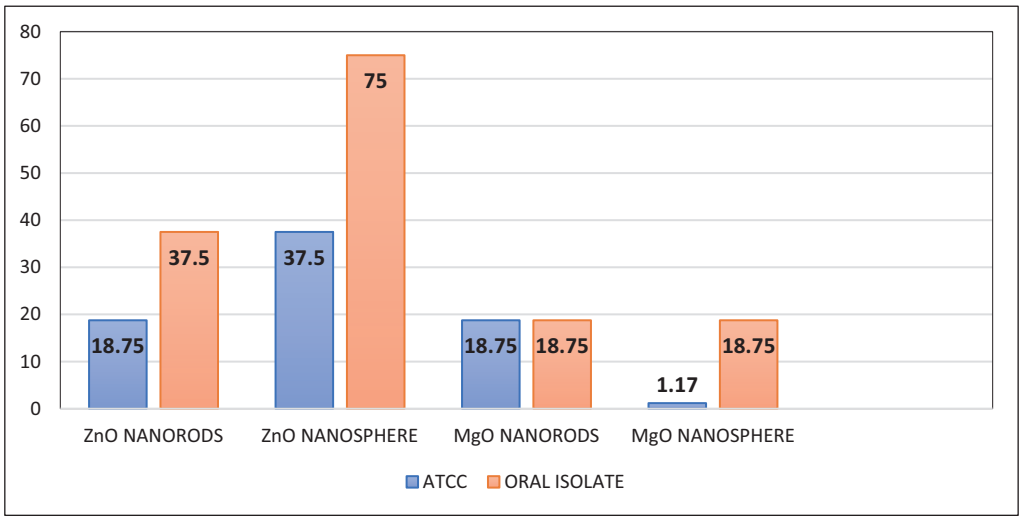

Graph 3: Minimum inhibitory concentration (mg/mL) of Nanoparticles against American-type culture collection and oral isolate strain

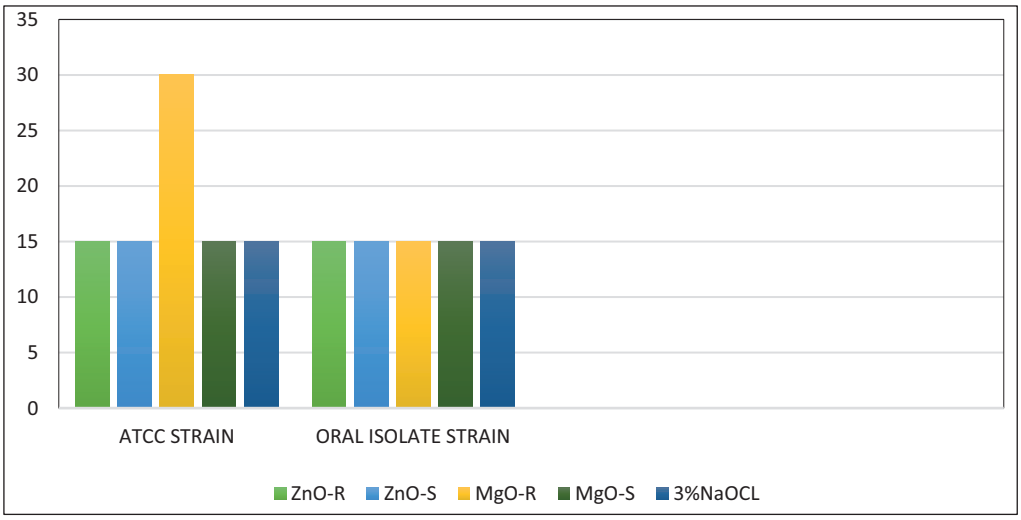

Graph 4: Time-kill assay of nanoparticles (in min) against American-type culture collection and oral isolate strain

Clinical isolate strain

It was found that MgO-R and MgO-S were effective at a concentration of 18.5 mg/mL, followed by ZnO-R at 37.5 mg/mL and ZnO-S at 75 mg/mL [Graph 3].

Time-kill assay

All of the NPs were shown to be effective against both strains in 15 min, which was comparable to 3% NaOCl. The exception was MgO-R, which showed bacterial growth against the ATCC strain in 15 min but killed the bacteria in 30 min [Graph 4].

Discussion

E. faecalis is consistently associated with root canal failures and cases of persistent apical periodontitis.[30] In addition, it exhibits a high level of resistance to a wide range of antimicrobial agents and is considered the prevalent organism in post-treatment infection.[31] This study aimed to determine the antibacterial efficacy of zinc oxide and magnesium oxide NPs (nanorod and nanosphere) against *E. faecalis*. An average particle size of 20 nm was synthesized and evaluated. The smaller size ensured efficient antimicrobial activity. The agar well diffusion test was employed to investigate the zone of inhibition of NPs comparing with 3% NaOCl (positive control) and 10% DMSO (negative control). Five distinct volumes such as 50, 75, 100, 125, and 150 µL were used to assess the antibacterial activity.

We observed that ZnO-R was effective against both strains of *E. faecalis* at 75 µL, while ZnO-S was effective only at higher volumes (100 µL for ATCC strain and 150 µL for oral isolates), respectively. Enhanced antimicrobial activity at lower volumes can be attributed to the morphology-dependent antimicrobial activity of ZnO NPs, with more facets on the surface indicating a higher antibacterial action.[32,33] ZnO-Rs have higher atomic density facets that make it easier to interact and penetrate bacterial cell walls more easily than spherical ZnO NPs.[34] In addition, increased yield of reactive oxygen species (ROS), such as superoxide anion (O_2), hydrogen peroxide (H_2O_2), and hydroxyl ion (OH^-), is responsible for the destroying of cellular contents, such as proteins, lipids, and nucleic acids, of the bacteria.[35] The effectiveness of ZnO-S at higher volumes can be attributed to variations in the synthesis of nanorods. Its antibacterial effectiveness is due to its activity on the cell walls of the organism, resulting in its damage and production of ROS, which disturbs the cellular metabolism. Furthermore, numerous research has demonstrated that when particle size decreased, antibacterial activity increased. As the size of the NPs lowers, their surface area increases, increasing their antibacterial activity.[36] This study used NPs with a lower size (20 nm) might have improved their antibacterial activity.

In this study, we found that MgO-R was efficient against the ATCC strain of *E. faecalis* at 100 µL but was effective at 125 µL against oral isolate strain. The antimicrobial action of MgO NPs is due to an increase in surface area and production of superoxide anion (O^{2-}) that interacts with peptide linkages and lipid peroxidation, and on the surface of NPs, there are numerous defects that take up halogen gases, which result in strong interaction with bacteria.[36,37] In addition, a decrease in particle size of MgO NPs is associated with increased antibacterial activity. According to Krishnamoorthy *et al.*,[37] the surface of MgO NPs may undergo successive oxidation-reduction events that result in the production of reactive oxygen species, including hydroxyl radical ($OH^·$), hydrogen peroxide (H_2O_2), and superoxide radical (O^{2-}). Defects or oxygen vacancies at the NP's surface also contribute to the mechanism of antibacterial action of magnesium oxide nanoparticles.[38] Another suggested mechanism of magnesium oxide NPs is the "alkaline effect." A thin layer of water that forms on

NPs as a result of moisture adsorption on their surface has an "alkaline pH," that is, greater than its equilibrium value in the solution. The high pH of the thin water layer on the surface causes membrane damage and cell death when the NPs come into contact with the bacteria.[39] It was found that MgO-S showed activity against the ATCC strain of *E. faecalis* at 125 µL but showed effectiveness against oral isolate at 100 µL. The mechanism underlying the antibacterial action of MgO nanosphere is similar to that of MgO nanorods. Additionally, it was shown that 50 µL of 3% NaOCl was effective against both strains. The activity of 3% NaOCl and ZnO-Rs was comparable. We also observed that the antibacterial activity of 3% NaOCl increased with an increasing volume of NPs against both ATCC and oral isolates, respectively. Considerable antibacterial activity was present in all NPs. The synthesis parameters, such as pH, calcination temperature, and chemical agents used, may be responsible for the difference in the antibacterial action of NPs.

The broth microdilution method was used to determine the MIC of NPs. Among the NPs, MgO-S was effective at a lesser concentration of 1.17 mg/mL, followed by MgO-R and ZnO-R, which were effective at 18.75 mg/mL, while ZnO-S was effective at a concentration of 37.5 mg/mL against ATCC 29212 strain. Against clinical isolate strain, MgO-R and MgO-S were effective at a concentration of 18.5 mg/mL, followed by ZnO-R at 37.5 mg/mL and ZnO-S at 75 mg/mL. This effectiveness of magnesium oxide NPs at lower concentrations could be due to the existences of numerous oxygen vacancies on the surface of the NPs.[37]

The time required for the NPs to kill the organisms was assessed using the time-kill assay. All of the NPs were successful against both strains in 15 min, comparable to 3% NaOCl, with the exception of the MgO-R, which showed bacterial growth against the ATCC strain in 15 min but killed the bacteria in 30 min. These NPs' rapid activity within 15 min could be attributed to the alkaline effect (MgO-nanorod and sphere), superoxide anion, and increased number of facets (ZnO nanorod and sphere). The produced NPs had an average size of 20 nm, which could have significantly improved and facilitated their antibacterial properties.

In this study, we found that 3% NaOCl had better scores that were consistently better at various concentrations. Nevertheless, de Almeida *et al*.[40] conducted an *in vitro* study and found 2% CHX superior to 3% NaOCl, silver nanoparticles (Ag NP), and ZnO Np, respectively. Though chemical agents, like NaOCl and CHX, are recommended and used extensively, NPs are often advocated to overcome the limitations of the above-mentioned chemical agents. NaOCl was found to be a better alternative than MgO Np in this study; however, an *ex vivo* study by Monzavi *et al*.[41] reported the latter to be more efficient in the long-term activity against *E. faecalis*. Ag NP is another class of NPs that have shown promising results due to their antimicrobial and anti-biofilm properties. These Ag NPs alter the bacterial cell permeability providing a safe passage for Ag ions to penetrate inside the bacteria and react with specific proteins, thereby resulting in cell death. A study by Wu *et al*.[42] revealed that 0.02% of Ag NP in gel form (as a medicament) could significantly reduce *E. faecalis* cells underscoring the mode of application of Ag NP.

The antimicrobial effect of Np can also be utilized when different NPs are added or coated over dental materials like gutta-percha or sealer. Panwar *et al*.[43] evaluated the antimicrobial efficacy of nanocurcumin against *E. faecalis* and found that nano curcumin-coated gutta-percha had a significantly higher zone of inhibition when compared to conventional gutta-percha, opening up newer avenues to explore the use of nanocurcumin as an inter-appointment medicament.

This initial investigation assessed the efficacy of two distinct NP morphologies to identify the variation in the antibacterial activity, that is, significantly impacted by their size and shape. Analysis of the cytocompatibility test of magnesium oxide and zinc oxide NPs, improvement of the NPs' surface properties through doping with appropriate substances, and the possibility of further investigation as a vehicle for bioactive substances would be the next big step in this research. This study has certain limitations, such as not being directly correlated to clinical scenarios and not being evaluated against polymicrobial biofilm as exist in clinical situations, and also needs to evaluate cytocompatibility assay for the NPs used.

Conclusion

Knowledge of the field of nanoscience could lead to new developments in endodontics. A new era in root canal system disinfection can be brought via the domain of nanotechnology, which achieves total root canal sterility and ensures the success of the endodontic procedure. In this study, magnesium oxide and zinc oxide nanoparticles with two distinct shapes, nanosphere and nanorod, were investigated against *E. faecalis*. All of the NPs demonstrated strong antibacterial activity, with ZnO-R demonstrating antibacterial activity on par with sodium hypochlorite. These NPs attracted significant attention due to their distinct characteristic features, which enable them to be used as a coating on gutta-percha surfaces and posts, as well as altered and integrated into endodontic materials like sealers, ultimately preventing post-treatment illnesses.

Acknowledgement

Not applicable.

Financial support and sponsorship

Nil.

Conflicts of interest
There are no conflicts of interest.

Authors' contributions
Not applicable.

Ethical policy and Institutional Review Board statement
Not applicable as *In-Vitro* Study.

Patient declaration of consent
Not applicable.

Data availability statement
Not applicable.

References

1. Haapasalo M, Shen Y, Qian W, Gao Y. Irrigation in endodontics. Dent Clin North Am 2010;54:291-312.
2. Mohammadi Z, Abbott PV. The properties and applications of chlorhexidine in endodontic: Review. Int Endod J 2009;42:288-302.
3. Rucucci D, Siqueira JF, Jr. Biofilms and apical periodontitis: Study of prevalence and association with clinical and histopathologic findings. J Endod 2010;36:1277-88.
4. Ferraz CC, Gomes BP, Zaia AA, Teixeira FB, Souza-Filho FJ. In vitro assessment of the antimicrobial action and the mechanical ability of chlorhexidine gel as an endodontic irrigant. J Endod 2001;27:452-5.
5. Jiang LM, Hoogenkamp MA, Van der Sluis LW, Wesselink PR, Crielaard W, Deng DM. Resazurin metabolism assay for root canal disinfectant evaluation on dual-species biofilms. J Endod 2011;37:31-5.
6. Jett BD, Huycke MM, Gilmore MS. Virulence of *Enterococci*. Clin Microbiol Rev 1994;7:462-78.
7. Peters OA, Laib A, Rüegsegger P, Barbakow F. Three-dimensional analysis of root canal geometry by high resolution computed tomography. J Dent Res 2000;79:1405-9.
8. Love RM. *Enterococcus faecalis*: A mechanism for its role in endodontic failure. Int Endod J 2001;34:399-405.
9. McHugh CP, Zhang P, Michalek S, Eleazer PD. pH required to kill *Enterococcus faecalis* in vitro. J Endod 2004;30:218-9.
10. Nair PN, Henry S, Cano V, Vera J. Microbial status of apical root canal system of human mandibular first molars with primary apical periodontitis after "one visit" endodontic treatment. Oral Surg Oral Med Oral Pathol Oral Radiol Endod 2005;99:231-52.
11. Siqueira JF, Jr, Rôças IN, Santos SR, Lima KC, Magalhães FA, de Uzeda M. Efficacy of instrumentation techniques and irrigation regimens in reducing the bacterial population within root canals. J Endod 2002;28:181-4.
12. Slutzky-Goldberg I, Maree M, Liberman R, Heling I. Effect of sodium hypochlorite on dentin microhardness. J Endod 2004;30:880-2.
13. Mohammadi Z. Sodium hypochlorite in endodontics: An update review. Int Dent J 2008;58:329-41.
14. Mohammadi Z, Giardino L, Mombeinipour A. Antibacterial substantivity of a new antibiotic-based endodontic irrigation solution. Aust Endod J 2012;38:26-30.
15. Bademela SL, Raju TB, Parvathaneni KP, Seshadri A, Varma NM, Dondapati GD. Comparison of penetration depth of chitosan, zinc oxide, and silica-doped titanium novel nanoparticle irrigant solutions – A confocal laser scanning microscopic in vitro study. Endodontology 2024;36:280-4.
16. Kishen A, Shi Z, Shrestha A, Neoh KG. An investigation on the antibacterial and antibiofilm efficacy of cationic nanoparticulates for root canal disinfection. J Endod 2008;34:1515-20.
17. Shrestha A, Kishen A. Antibacterial nanoparticles in endodontics: A review. J Endod 2016;42:1417-26.
18. Gutierrez FM, Olive PL, Banuelos A, Orrantia E, Nino N, Sanchez EM, *et al*. Synthesis, characterization, and evaluation of antimicrobial and cytotoxic effect of silver and titanium nanoparticles. Nanomedicine 2010;6:681-8.
19. Jhamb S, Singla R, Kaur A, Sharma J, Bhushan J. In vitro comparison to study the antimicrobial effect of silver nanoparticles gel and its various combinants as an intracanal medicament against *Enterococcus faecalis*. J Conserv Dent Endod 2024;27:42-5.
20. Balsaraf O, Raghavendra SS, Shah D, Sanjyot M, Balsaraf A. Comparative evaluation of antifungal efficacy of conventional endodontic irrigants and chitosan nanoparticles. J Conserv Dent 2023;26:226-9.
21. Kishen A, Peters OA, Zehnder M, Diogenes AR, Nair MK. Advances in endodontics: Potential applications in clinical practice. J Conserv Dent 2016;19:199-206.
22. Panahandeh N, Torabzadeh H, Aghaee M, Hasani E, Safa S. Effect of incorporation of zinc oxide nanoparticles on mechanical properties of conventional glass ionomer cements. J Conserv Dent 2018;21:130-5.
23. Pandiyan I, Sri SD, Indiran MA, Rathinavelu PK, Prabakar J, Rajeshkumar S. Antioxidant, anti-inflammatory activity of *Thymus vulgaris*-mediated selenium nanoparticles: An in vitro study. J Conserv Dent 2022;25:241-5.
24. Wei H, Wu Y, Lun N, Hu C. Hydrothermal synthesis and characterization of ZnO nanorods. Mater Sci Eng A 2005;393:80-2.
25. Sarkar S, Sarkar R. Sol-gel synthesis and meticulous characterization of zinc oxide nanoparticles. J Nanosci Curr Res 2017;2:109-12.
26. Alaei M, Jalali M, Rashidi A. Simple and economical method for the preparation of MgO nanostructures with suitable surface area. Iran J Chem Chem Eng 2014;33:21-8.
27. Wahab R, Absari SG, Dar MA, Kim YS, Shin HS. Synthesis of magnesium oxide nanoparticles by sol-gel process. Mater Sci Forum Vols 2007;558:983-6.
28. Nkemzi AQ, Okaiyeto K, Oyenihi O, Opuwari CS, Ekpo OE, Oguntibeju OO. Antidiabetic, anti-inflammatory, antioxidant, and cytotoxicity potentials of green-synthesized zinc oxide nanoparticles using the aqueous extract of *Helichrysum cymosum*. 3 Biotech 2024;14:291.
29. Geethapriya N, Subbiya A, Padmavathy K, Mahalakshmi K, Vivekanandan P, Sukumaran VG. Effect of chitosan ethylenediamine tetra-acetic acid on *Enterococcus faecalis* dentinal biofilm and smear layer removal. J Conserv Dent 2016;19:472-7.
30. Haapasalo M, Ranta H, Ranta KT. Facultative gram-negative enteric rods in persistent periapical infections. Acta Odontol Scand 1983;41:19-22.
31. Rôças IN, Siqueira JF, Santos KR. Association of *Enterococcus faecalis* with different forms of periradicular diseases. J Endod 2004;30:315-20.
32. Rago I, Chandraiahgari CR, Bracciale MP, De Bellis G, Zanni E, Guidi MC, *et al*. Zinc oxide microrods and nanorods: Different antibacterial activity and their mode of action against gram-positive bacteria. RSC Adv 2014;4:56031-40.
33. Ramani M, Ponnusamy S, Muthamizhchelvan C, Marsili E. Amino acid-mediated synthesis of zinc oxide nanostructures and evaluation of their facet-dependent antimicrobial activity. Colloids Surf B Biointerfaces 2014;117:233-9.
34. Sawai J. Quantitative evaluation of antibacterial activities of metallic oxide powders (ZnO, MgO and CaO) by conductimetric assay. J Microbiol Methods 2003;54:177-82.
35. Zhang L, Jiang Y, Ding Y, Povey M, York D. Investigation into the antibacterial behaviour of suspensions of ZnO nanoparticles (ZnO nanofluids). J Nanopart Res 2007;9:479-89.
36. Raghupathi KR, Koodali RT, Manna AC. Size-dependent bacterial growth inhibition and mechanism of antibacterial activity of zinc oxide nanoparticles. Langmuir 2011;27:4020-8.

37. Krishnamoorthy K, Manivannan G, Kim SJ, Jeyasubramanian K, Premanathan M. Antibacterial activity of MgO nanoparticles based on lipid peroxidation by oxygen vacancy. J Nanopart Res 2012;14:1063-6.
38. Leung YH, Ng AM, Xu X, Shen Z, Gethings LA, Wong MT, *et al*. Mechanisms of antibacterial activity of MgO: Non-ROS mediated toxicity of MgO nanoparticles towards Escherichia coli. Small 2014;10:1171-83.
39. Tang Z-X, Lv B-F. MgO nanoparticles as antibacterial agent: Preparation and activity. Braz J Chem Eng 2014;31:591-6.
40. de Almeida J, Cechella BC, Bernardi AV, de Lima Pimenta A, Felippe WT. Effectiveness of nanoparticles solutions and conventional endodontic irrigants against *Enterococcus faecalis* biofilm. Indian J Dent Res 2018;29:347-51.
41. Monzavi A, Eshraghi S, Hashemian R, Momen-Heravi F. In vitro and ex vivo antimicrobial efficacy of nano-MgO in the elimination of endodontic pathogens. Clin Oral Invest 2014;19:349-56.
42. Wu D, Fan W, Kishen A, Gutmann JL, Fan B. Evaluation of the antibacterial efficacy of silver nanoparticles against *Enterococcus faecalis* biofilm. J Endod 2014;40:285-90.
43. Panwar D, Sidhu K, Bhushan J, Kakkar V, Mehta M, Sharma J. Evaluation of antimicrobial efficacy of nanocurcumin-coated gutta-percha against *Enterococcus faecalis*: An *in vitro* study. J Conserv Dent 2023;26:160-4.

Supplementary Data

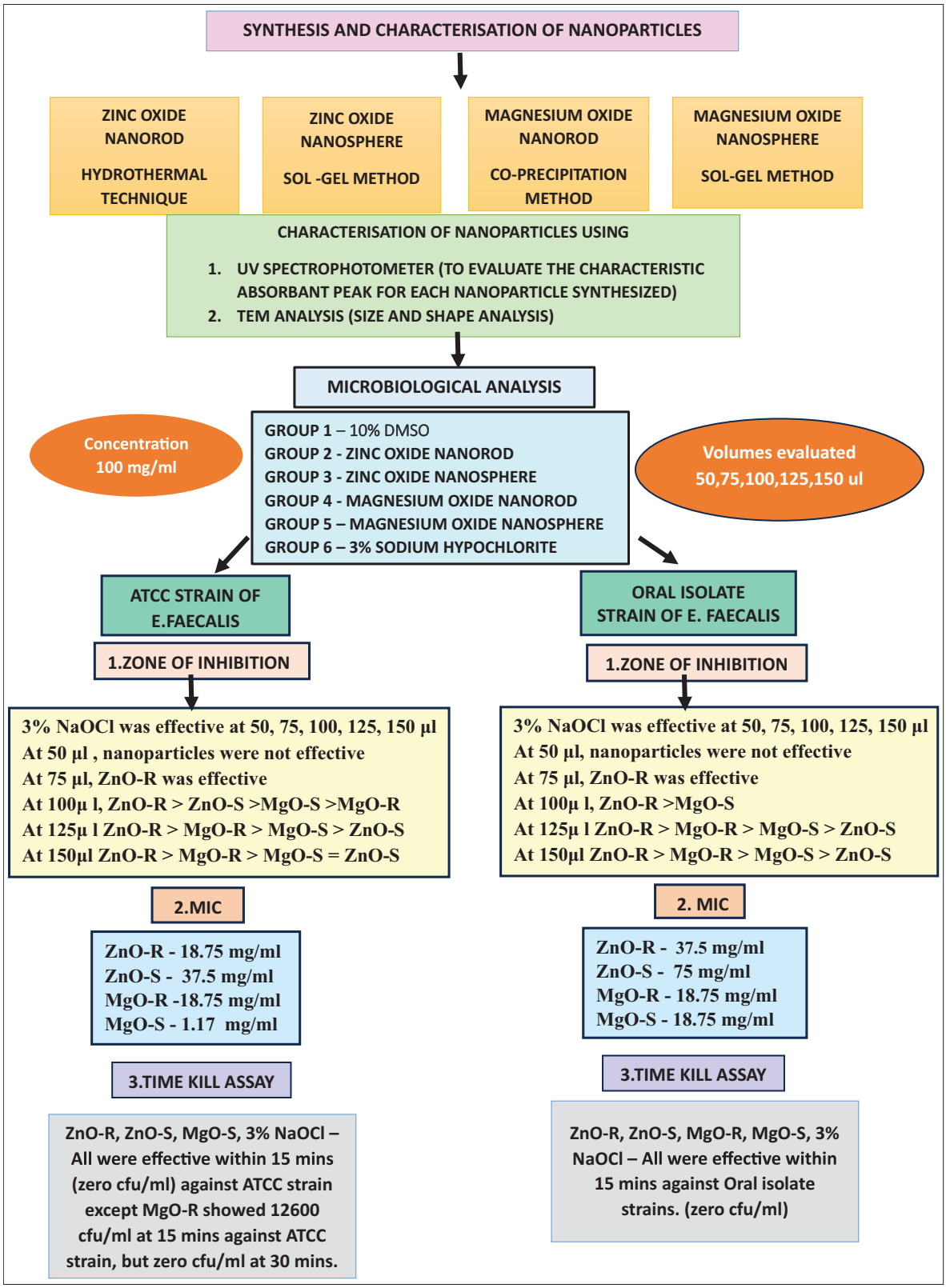

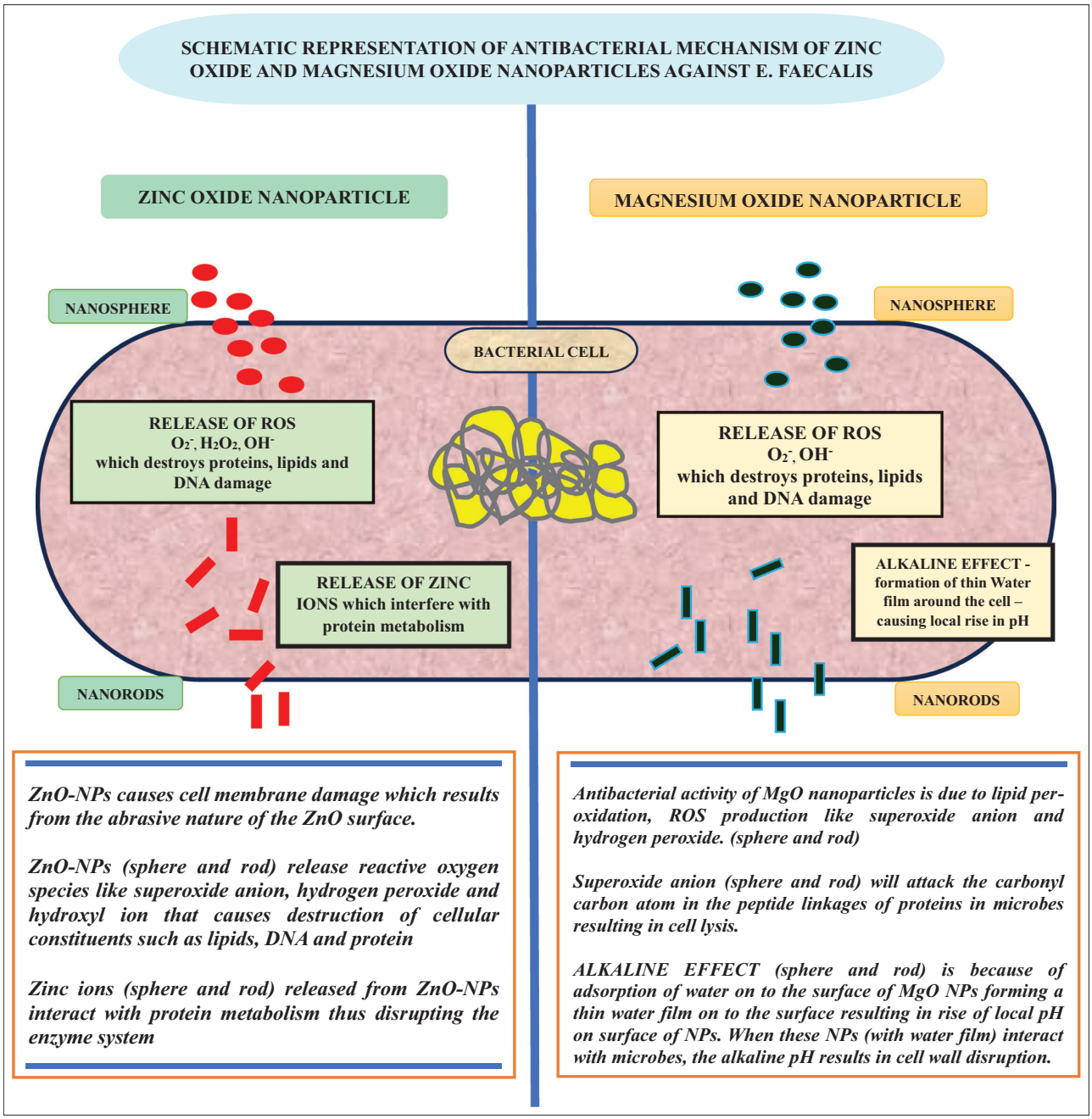
SCHEMATIC REPRESENTATION OF ANTIBACTERIAL MECHANISM OF ZINC OXIDE AND MAGNESIUM OXIDE NANOPARTICLES AGAINST E. FAECALIS
ZINC OXIDE NANOPARTICLE
MAGNESIUM OXIDE NANOPARTICLE
NANOSPHERE
NANOSPHERE
BACTERIAL CELL
RELEASE OF ROS O_2^-, H_2O_2, OH^- which destroys proteins, lipids and DNA damage
RELEASE OF ROS O_2^-, OH^- which destroys proteins, lipids and DNA damage
RELEASE OF ZINC IONS which interfere with protein metabolism
ALKALINE EFFECT - formation of thin Water film around the cell – causing local rise in pH
NANORODS
NANORODS
ZnO-NPs causes cell membrane damage which results from the abrasive nature of the ZnO surface.
ZnO-NPs (sphere and rod) release reactive oxygen species like superoxide anion, hydrogen peroxide and hydroxyl ion that causes destruction of cellular constituents such as lipids, DNA and protein
Zinc ions (sphere and rod) released from ZnO-NPs interact with protein metabolism thus disrupting the enzyme system
Antibacterial activity of MgO nanoparticles is due to lipid peroxidation, ROS production like superoxide anion and hydrogen peroxide. (sphere and rod)
Superoxide anion (sphere and rod) will attack the carbonyl carbon atom in the peptide linkages of proteins in microbes resulting in cell lysis.
ALKALINE EFFECT (sphere and rod) is because of adsorption of water on to the surface of MgO NPs forming a thin water film on to the surface resulting in rise of local pH on surface of NPs. When these NPs (with water film) interact with microbes, the alkaline pH results in cell wall disruption.